

Effects of design parameters and A_f temperature on superelastic behaviour of Nitinol stent for application in biliary duct: finite element analysis

F. Nematzadeh*¹ and S. K. Sadrnezhad²

For more than a decade, stent implantation has been strategically used for solving gastrointestinal dilemmas such as biliary stenosis. Predicaments like insufficient radial strength, low twisting ability, inappropriate dynamic behaviour and restenosis are expected to be solved by the introduction of new designs. Superelastic Nitinol stent is an interesting alternative for minimising these tight spots. The application of finite element method to predict metallurgical and geometric behaviour of superelastic Nitinol stents for biliary duct dilatation is supported by conventional crimp tests. Model calculations show that all stents encounter the highest stress in their intersegment curvature. Inner curvature can, thus, be considered as the most critical segment with the highest frequency of martensite assessment. Owing to lower chronic outward force, higher radial resistive force and more suitable superelastic behaviour, Nitinol stents with optimal A_f temperature of 24°C and intersegment angle of 65° are shown to have the best mechanical performance for clinical applications. Moreover, model calculations show that a 1° change in stent intersegment and 2°C change in A_f temperature can substantially influence the mechanical performance of the stent.

Keywords: Finite element analysis, Nitinol stent, Biliary duct, Design parameters, A_f temperature

Introduction

A major cause of death throughout the world is gastrointestinal disease.¹ Biliary obstruction is the most well known gastrointestinal ailment.² Malignant biliary obstruction causes jaundice, frequently accompanied with pruritus. Stent placement has been used as a main solution to this hitch during past decade.^{3–6} The application of stent has two main objectives: preventing short term effects of intimal dissection and elastic recoil and preventing long term effects like restenosis due to the neointimal hyperplasia. Successful employment of stent is bound to the following conditions: good controllability to obtain an adequate fixation to the duct wall; adequate resistance against the elastic recoil; resistance to fatigue owing to the pulsatile flow on body kinematics; size minimisation of the device for easier percutaneous procedure; low thrombogenicity; acceptable biocompatibility and long term palliation of patients from malignant obstructive jaundice.

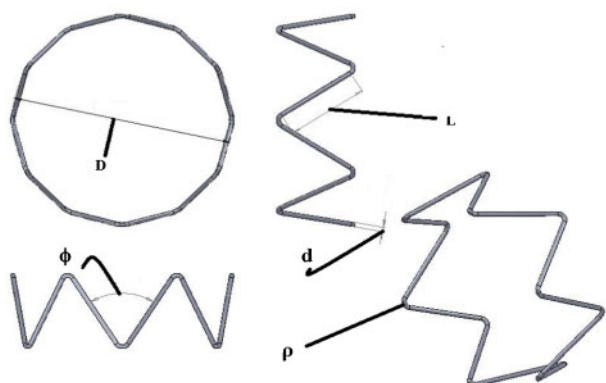
Different geometries like coil, helical spring, woven (braided and knitted), ring (individual and sequential) and cells (closed and open) have been already used for stents.⁵ Wire based stents are designed for non-vascular applications. Their advantage is flexibility and retrievability. A newer design is ZA biliary stents⁶ having clinical usage with preselected radial force. It can be used as an experimental model for determining the effect of surface area and the radial force on the biological response. Although the transformation of the radial force seems desirable, this does not seem practicable with the current generation of commercially available stents. The Z shape provides a convenient model for the production of customised stents because of the ease with which it can be manufactured. This shape permits alternative designs for the investigation of the effect of different parameters on radial forces. A method has also been developed for the prediction of the radial forces for the Z shape stents based on the Castigliano's second theorem.⁷

Considerations have recently been given to the utilisation of Nitinol alloy for devising newly developed stents. Whitcher⁸ numerically studied the fatigue behaviour of Nitinol in order to use it in the manufacture of the stents. Petrini *et al.*⁹ developed a numerical model for the explanation of the stent crushing test results.

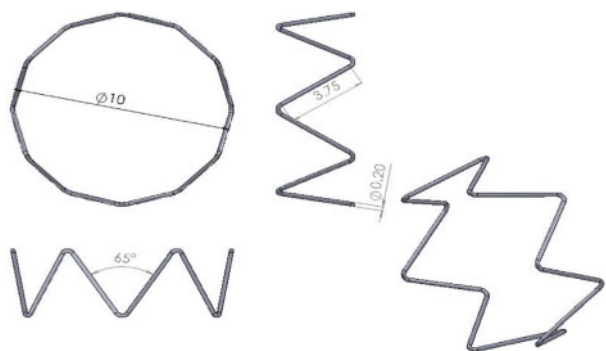
¹Department of Materials Engineering, Faculty of Engineering, Arak University Arak, PO Box 38156-88349, Iran

²Department of Materials Science and Engineering, Sharif University of Technology, PO Box 11155-9466, Tehran, Iran

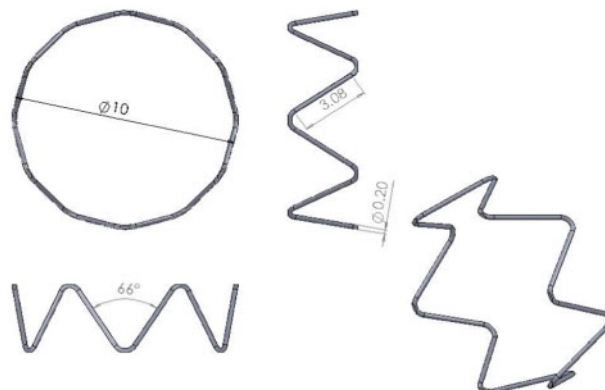
*Corresponding author, email fardinnematzadeh@gmail.com



1 Geometric parameters of Z shape biliary stent



2 Z shape biliary stent with bending angle of 65° (unit of length is mm)



3 Z shape biliary stent with bending angle of 66° (unit of length is mm)

model is developed based on the non-linear 3D finite element method. It is capable of determining the mechanical and clinical performance of the superelastic Nitinol wire stents implantable in the common bile ducts.

Materials and research method

Geometric model and material properties

For designing Nitinol biliary stent of this research, important parameters included shape, length, angle and curvature of the segments and diameter and A_f temperature of the utilised superelastic wire. The effects of the length and angle of the segments and A_f temperature of the alloy were investigated, while other parameters were assumed constant. The Z shape geometric models needed for the simulation of the biliary stents were generated by computer aided three-dimensional interactive application (CATIA V.5; Dassault Systèmes, USA) on the basis of the available clinical reports^{3,4,18} and then, were transformed into the finite element analysis code Abaqus 6-10 (Dassault Systèmes, Providence, RI, USA).

Geometric parameters of the Z shape biliary stent are as sketched in Fig. 1 and quantified in Table 1, Figs. 2 and 3. Geometric parameters shown in Figs. 2 and 3 were based on age treatment of Ti-50.7%Ni alloy at 500°C for respective durations of 60 and 30 min according to the clinical reports given in the literature.^{3,4,18} Different views for better understanding of the meshing are shown in Fig. 4. Works of Auricchio, Taylor and Lubliner with extensive extensions of Rebelo^{10,23-29} were used to develop the Abaqus Nitinol model which employed superelastic behaviour as a predefined material condition.

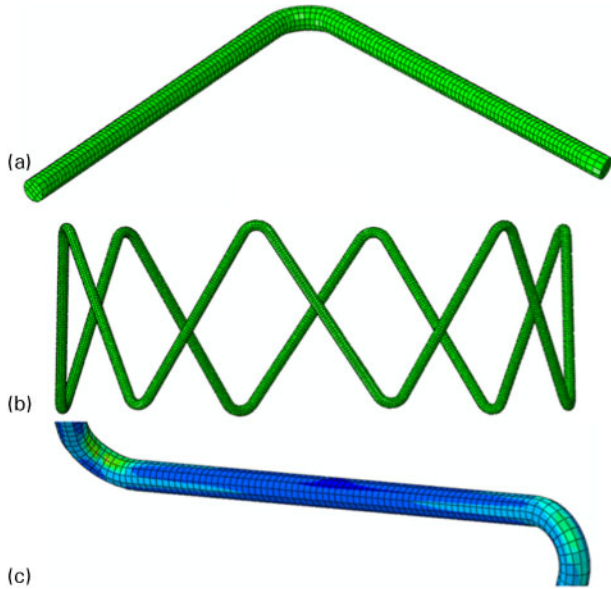
The model first developed by Auricchio *et al.* and Lubliner *et al.* and then, extensively extended by Rebelo *et al.* is used for the simulation of Nitinol superelastic behaviour.²³⁻²⁷ The model is based on the generalisation of the theory of plasticity and the second law of thermodynamics written in terms of Helmholtz free energy. In this theory, strain is decomposed into two components

Kleinstreuer *et al.*¹⁰ mathematically analysed superelastic behaviour of different Nitinol graft stents designed for supporting abdominal aortic aneurysm. Merwe *et al.*¹¹ used finite element analysis for designing knitted Nitinol meshes for prospective application as external vein reinforcement. De Beule *et al.*¹² optimised mechanics of braided stents. Silber *et al.*¹³ worked on the effect of stent geometrical characteristics on the mechanical properties of Nitinol wire stents. Numerical investigation of Z shape Nitinol stents for biliary duct seems, however, missing in the literature.

Previous studies have shown that A_f temperature has a significant influence on the mechanical and clinical performance of self-expanding Nitinol stents.^{6,9,14-19} Although several authors have analysed the general forces that Nitinol wire stents exert,^{8,10,12,13,20-22} no data are available on force-displacements of Z shape Nitinol stents. The present study provides a comprehensive evaluation of the effect of segment length, angle and A_f temperature on the mechanical performance of Z shape Nitinol stents when supposedly used in the bile duct of the liver. The effects of the influential parameters are predicted via model calculations and verified by the empirical information available in the literature. The

Table 1 Geometric values for stents of this research

Samples	Internal diameter of stent D /mm	Radius of curvature ρ	Segment length L /mm	Diameter of wire d /mm	Bending angle ϕ
Figure 2	10.0	0.3	3.75	0.2	65°
Figure 3	10.0	0.3	3.08	0.2	66°



a studied part of stent; b complete stent; c exact position of stent where numerical calculations are performed
4 Different views are shown for better understanding of meshing: mesh density is 127 elements and 1020 nodes per mm²

$$\Delta\varepsilon = \Delta\varepsilon^{el} + \Delta\varepsilon^{tr} \tag{1}$$

where $\Delta\varepsilon^{el}$ is the elastic strain and $\Delta\varepsilon^{tr}$ is the transformation strain. Austenite is transformed into twinned martensite caused by the motion of shear forces which takes place in the stress threshold range of the superelastic material according to the following equations

$$F^S \leq F \leq F^F \tag{2}$$

where F is the transformation potential and S and F denote the martensite transformation start and finish temperatures respectively

$$\Delta\varepsilon^{tr} = a\Delta\zeta \frac{\partial F}{\partial \sigma} \tag{3}$$

$$\Delta\zeta = f(\sigma, \zeta)\Delta F \tag{4}$$

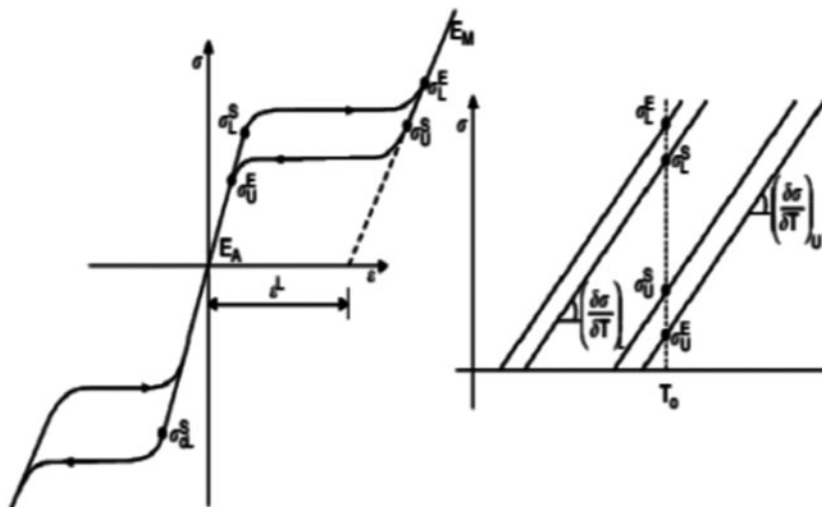
$$F = \bar{\sigma} - p \tan \beta + CT \tag{5}$$

where a is the coefficient of strain, ζ is the martensite fraction, σ is the von Mises stress, $\bar{\sigma}$ is the von Mises equivalent stress, p is the pressure, β and C are the material constants and T is the temperature. Similar approach is applied to define reverse transformation which takes different stress thresholds into account. Equations (3) and (4) define the transformation intensity. Any change in stress direction generates a martensite reorientation with negligible additional attempt. Furthermore, the model includes linear shifting of stress thresholds with temperature. In view of the fact that there is a volume increase associated to transformation, less stress is needed to generate transformation in tension and specifically in compression. This effect is modelled by linear Drucker–Prager approach for the transformation potential shown in equation (5) mentioned by Rebelo *et al.*²⁵ Figure 5 illustrates the typical behaviour of superelastic Nitinol alloy. The basis for material property selection of the stents is age treatment results of the Ti–50.7%Ni alloy at 500°C for 30 and 60 min durations. The data given for sample No. 1 of Table 2 are based on age treatment of Ti–50.7%Ni alloy at 500°C for 30 min.¹⁸ The data of the sample No. 2 of Table 2 are based on age treatment of Ti–50.7%Ni alloy at 500°C for 60 min.¹⁸ Parameters required in Abaqus user material subroutine for Nitinol material are summarised in Table 2.^{18,30–35} Before testing, a cubic element of Nitinol was considered and simulation results were compared with the experimental data.

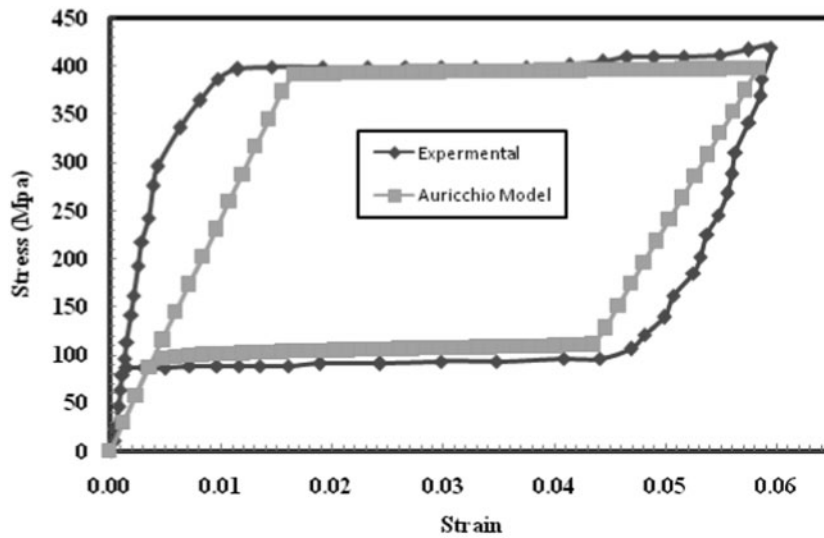
Comparison of different models confirmed better fit of the Auricchio model with the available empirical information (Figs. 6 and 7). The Auricchio model was, hence, selected for the determination of the properties used in stent modelling of this research.

Hypermesh (Altair Hypermesh v. 6.0) is a high performance finite element preprocessor that provides highly interactive software for performance analysis of product design. It is noticeable that Hypermesh software is used to mesh the samples owing to the mesh problems caused by small section of the Nitinol wire and relatively complex geometry of the stents.

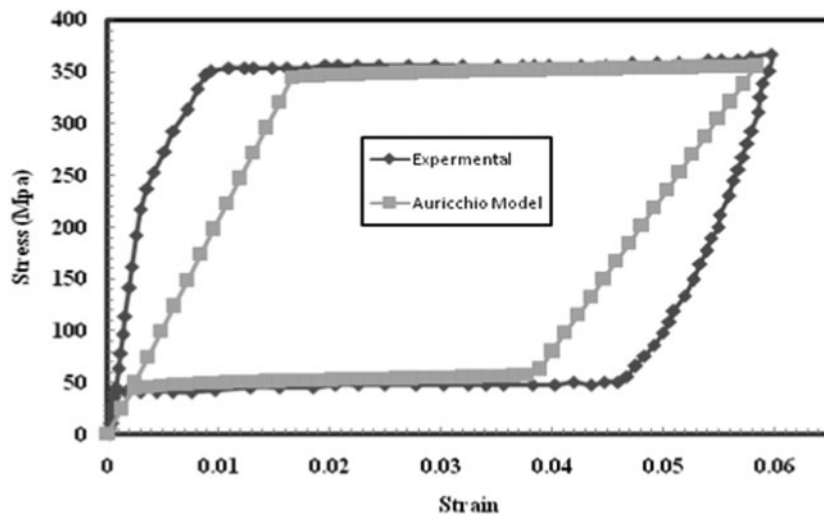
Mesh parameters are listed in Table 3. The incompatible mode eight node brick element C3D8I is an improved version of the standard solid eight node brick element C3D8 which was used in this work for solving shear locking, bending and contact of the stent. The



5 Superelastic behaviour of typical Nitinol wire¹⁰



6 Comparison of Auricchio model results with experimental data of superelastic Nitinol sample No. 1 of Table 2

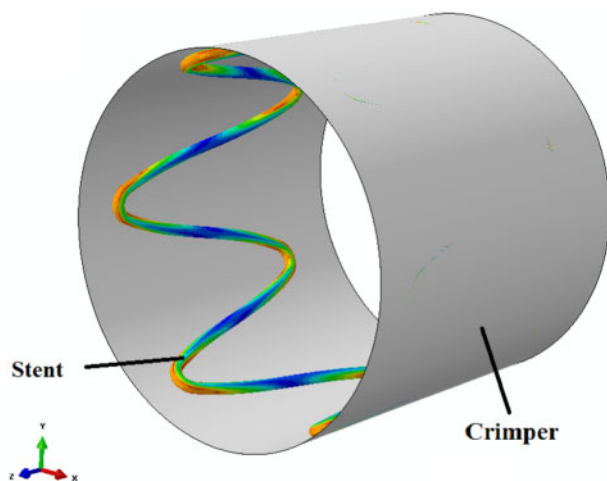


7 Comparison of Auricchio model results with experimental data of superelastic Nitinol sample No. 2 of Table 2

Table 2 Properties of Ni-Ti alloy used for biliary duct opening stents of this research*

Material property	Sample No. 1	Sample No. 2
Austenite elasticity E_A /MPa	24 100	20 700
Austenite Poisson's ratio ν_A	0.33	0.33
Martensite elasticity E_M /MPa	17 800	11 700
Martensite Poisson's ratio ν_M	0.33	0.33
Transformation strain ϵ^L	0.054	0.055
Loading $(\delta\sigma/\delta T)_L$ /MPa T^{-1}	5.32	5.32
Start of transformation loading σ_L^S /MPa	390	344
End of transformation loading σ_L^E /MPa	401	363
Reference temperature T_0 /°C	37	37
Unloading $(\delta\sigma/\delta T)_U$ /MPa T^{-1}	5.32	5.32
Start of transformation unloading σ_U^S /MPa	112	58
End of transformation unloading σ_U^E /MPa	93	42
Start of transformation stress in compression σ_{CL}^S /MPa	0.0	0.0
Volumetric transformation strain ϵ_V^L	0.054	0.055
A_f temperature/°C	22	24
Segments bending angle	66	65

*The data are based on the Auricchio model.^{18,30-35}



8 Crimper boundary of biliary Nitinol stent

strain energy release rates obtained from the model using C3D8I elements in comparison with C3D8 element are in excellent agreement with the values from the experimental works and the previous analyses given in the literature.³⁶ Also, the surface four node 3D linear quadrilateral thin element (SFM3D4) used in this research has no inherent stiffness and behaves just like the membrane elements.

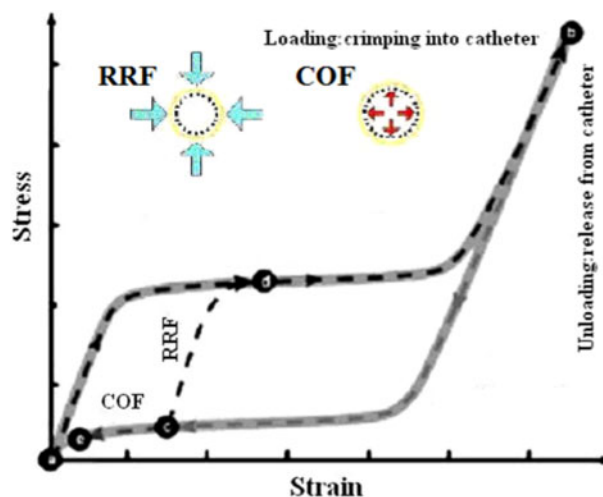
Crimping test

Contacts between the outer stent surface and the inner crimper surface were only activated during ABAQUS/STD contact module utilisation. Contact algorithm simultaneously applied the master surface precedence to the crimping test results as the stent was set for the slave surface. Penalty is a general method for the evaluation of the contact with friction coefficients different in ABAQUS analysis. Such a contact is used to enforce impermeable boundaries. It is assumed hard and frictionless. The penalty method allows superposition and then, assesses a penalty to push the faces apart. Boundary conditions were selected so as to avoid the sliding of the stent among the cylindrical surfaces as well as to allow the stent deformation during crimping. The rotation of all components was, thus, inhibited. While the stent was fixed in axial direction at its end nodes, the radial direction of the stent was allowed to deform without restraint under the crimping conditions. A radial displacement was enforced to the crimper that was recovered after the unloading towards the original status.^{10,13,37–41} A 60% diameter reduction was applied to the cylindrical surface of the stent. Boundary conditions for crimping of the biliary Nitinol stent are shown in Fig. 8.

The temperature was adjusted at normal body temperature (37°C). During crimping, self-contact (between the edges of the stent) behaviour was anticipated. This could impose additional stress on the contact interfaces. Owing to the superelastic behaviour of the stent, these

Table 3 Mesh parameters for crimping test of biliary stent

Material	Element type	Number of elements	Number of nodes
Stent	C3D8I	14 400	18 900
Crimper	SFM3D4	128 160	128 961



9 Schematics of RRF and COF for superelastic Nitinol stent^{6,44}

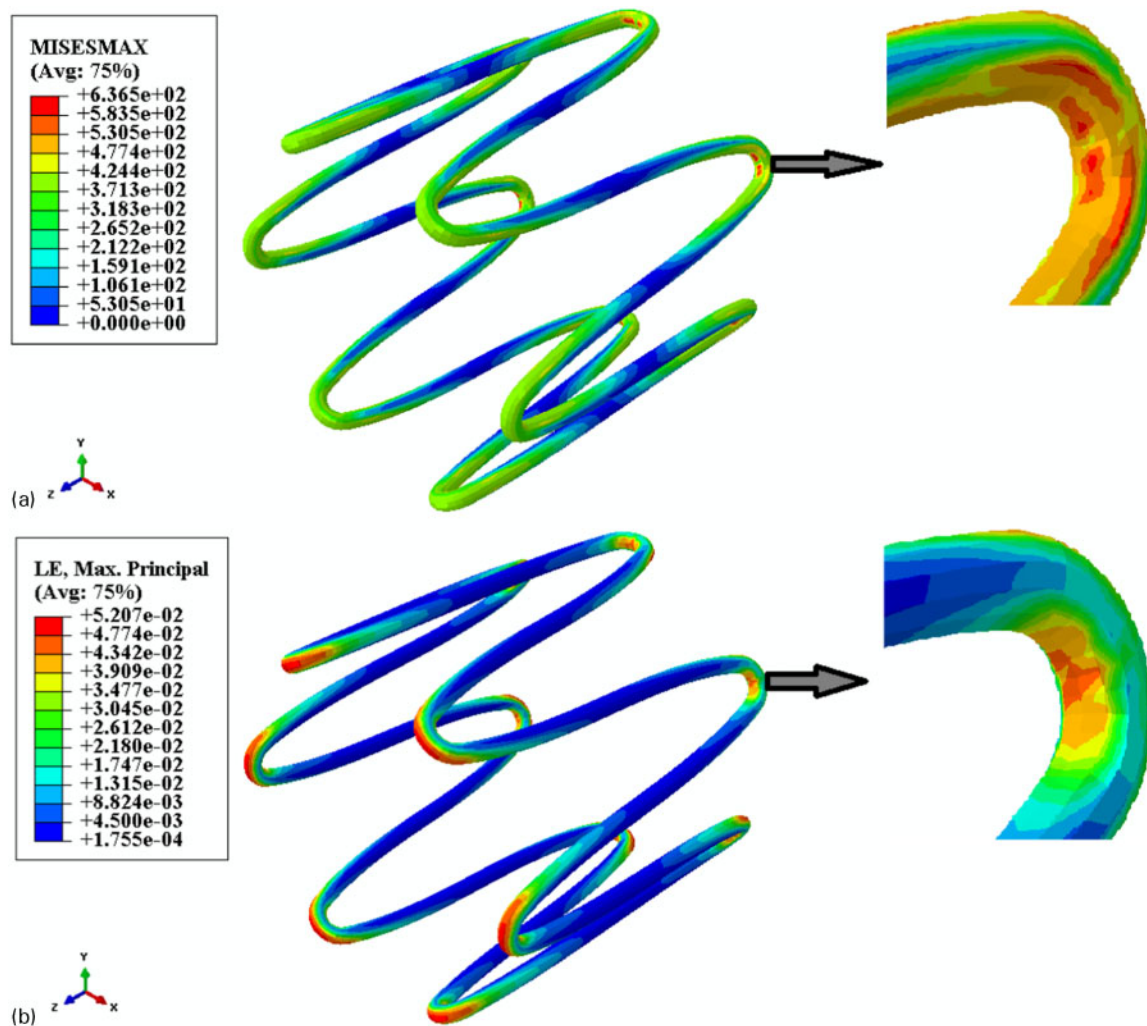
stresses for simplicity could, however, be neglected.³⁹ The procedure was, in fact, too complicated owing to the non-linear geometry, multiple interfaces, huge deformation, material nonlinearity, additional buckling and frequent bending of the stent.

Results and discussion

Parameters affecting the performance of Nitinol stent are superelasticity, force–displacement hysteresis, chronic outward force (COF), radial resistive force (RRF), distribution of stress and strain, plateau stress and the percentage of martensite phase.^{5,6,13,23} Desirable Nitinol stents require low COF, high RRF, wide stress plateau, full hysteresis loop, small localised stress, large superelastic strain and large martensitic phase.^{5,6,10,11,13,23,42,43} The COF and RRF depend on superelastic behaviour of the Nitinol stent. A classic superelastic stress–strain curve of a self-expanding stent is illustrated in Fig. 9. The stent is crimped at cylindrical surface (path a – b), next deployed to obtain stress equilibrium with the duct at point c . The force against the duct is controlled by the COF (ce) and the resistance against deformation by the RRF (d). Stent designers make effort, generally, for as high as possible RRF with as low as possible COF.^{6,44} Two particular points should be considered: the stents are never conditioned in the elastic region and their superelastic properties ought to be satisfactorily available on the basis of the need for flexible coils at the failure safe domains.^{6,16,45,46}

There are several parameters for the geometric design of the stent describing its mechanical properties.^{6,8,12} These parameters are: stent length, stent inner diameter, stent chord diameter, stent turning number, segments angle and stent radial contraction. Based on previous numerical studies,^{10,12,13,36,46–49} higher inner and chord diameters, segment angles and stent radial contractions result in superior performance of the superelastic Nitinol stents. Higher length and turning number of the stents has negative effect owing to poor superelasticity behaviour.

Previous researchers have indicated significant influence of the martensite/austenite transformation temperatures (especially A_f) on appropriate performance of Nitinol superelastic stents.^{14–16,21,50,51} The A_f temperature of the utilised Nitinol should be lower than the



a maximum von Mises stress; b maximum principal strain

10 Result of 60% crimping induced on biliary stent made with sample No. 1 of Table 2 having 66° angle between successive segments

normal body temperature so that the Nitinol stent preserves its superelastic behaviour.^{6,10,14-19,50,51} The magnitude of A_f is chosen on the basis of the stiffness and obstruction level of the duct. An A_f close to the body temperature is not desirable for lofty obstructions which need high RRF. Duct stenosis with little or no obstruction requires low stiffness and an A_f close to the normal body temperature. In the case of duct stenosis with large obstruction, stents with A_f temperatures much lower than the normal body temperature are required in order to supply enough radial strength for desirable duct opening performance.

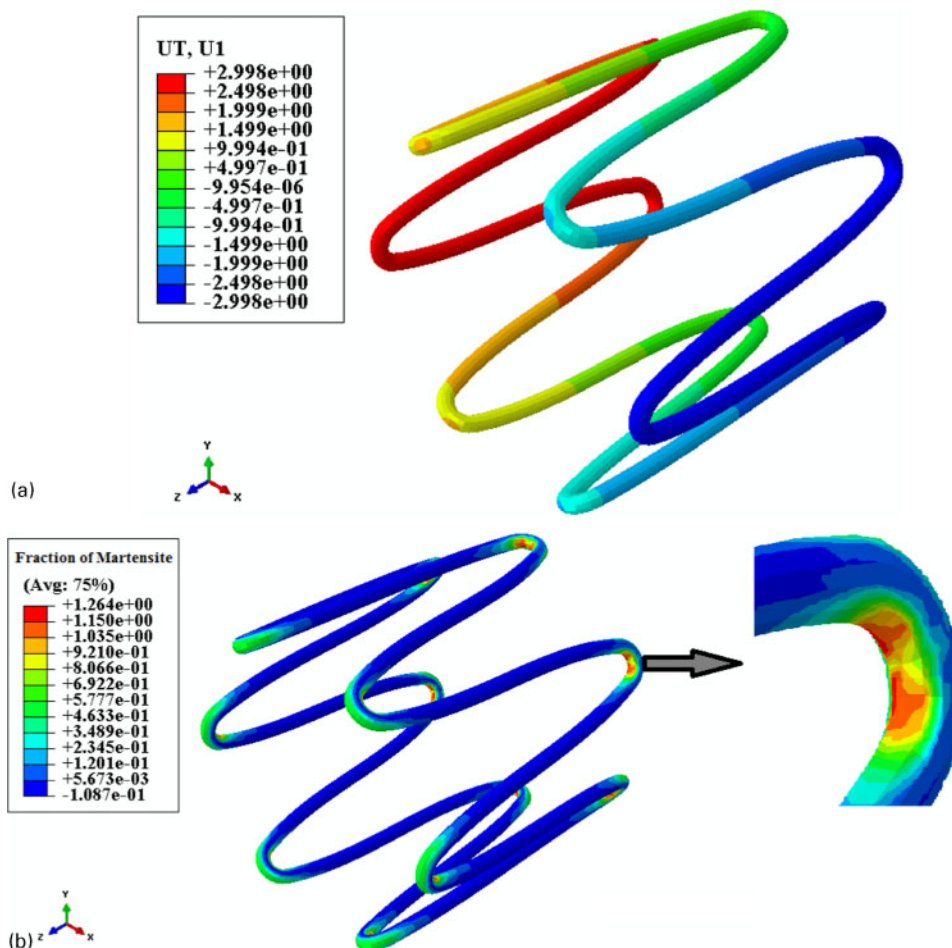
Very low A_f temperatures are not recommended because of the possibility of damaging the duct wall due to large radial strength and high stiffness. Greater toughness results in more cyclic strain endurance and longer fatigue life of Nitinol under tensile and compressive cyclic loads. To achieve desirable superelastic behaviour with the consideration of safety precautions against fracture, one can select Nitinol stents with lower A_f , lower fatigue life and higher strength or larger A_f with longer fatigue life and lower strength. Nitinol stents with high A_f temperatures (close to the body temperature) show, however, lower COF. Nitinol stents with acceptable performance in terms of low obstruction of biliary ducts do not require high RRF. The A_f

temperature of the Nitinol stents for highly obstructed biliary ducts should be well below the body temperature owing to the high RRF needed.

The use of Z shape geometry with Nitinol wire for making biliary stents is a new idea originally used in this research. Because of the lack of literature data, comparison of the performance of the newly developed stents with the traditional ones was not possible. Nitinol stents designed for biliary ducts were, however, examined by crimping test. The study was focused on the properties of the superelastic Nitinol wire and the geometric characteristics of the stents designed for clinical applications. It was shown that higher A_f temperature and lower length and angle of the stent segments can drastically improve the mechanical and clinical performance of the biliary Nitinol stents.

Maximum amounts of von Mises yield stress, principal strain, radial displacement and martensite fractional conversion caused by 60% crimping of Nitinol stents having 66° angle, and material properties specified by sample No. 1 of Table 2, are shown in Figs. 10 and 11. Similar plots for sample 2 of Table 2 are shown in Figs. 12 and 13.

Comparison of Figs. 10 and 12 indicates that the decrease in the maximum stress from 636.5 to 460.4 MPa results in an insignificant increase in the



a radial displacement; b fraction of martensite

11 Result of 60% crimping induced on biliary stent made with sample No. 1 of Table 2 having 66° angle

maximum strain from 0.052 to 0.0526. This increasing ratio is $\sim 1.15\%$.

Since the maximum stress induced on internal curvature of the stent depicted in Fig. 10a is larger than that of Fig. 12a, the latter is preferred to the former when considering the mechanical and clinical design aspects of these stents for the use in biliary ducts. Since the maximum strain induced on the internal curvature of the stent illustrated in Fig. 11b is lower than that of Fig. 13b, the latter possesses better dynamic motion and is in greater harmony with the biliary duct conditions.

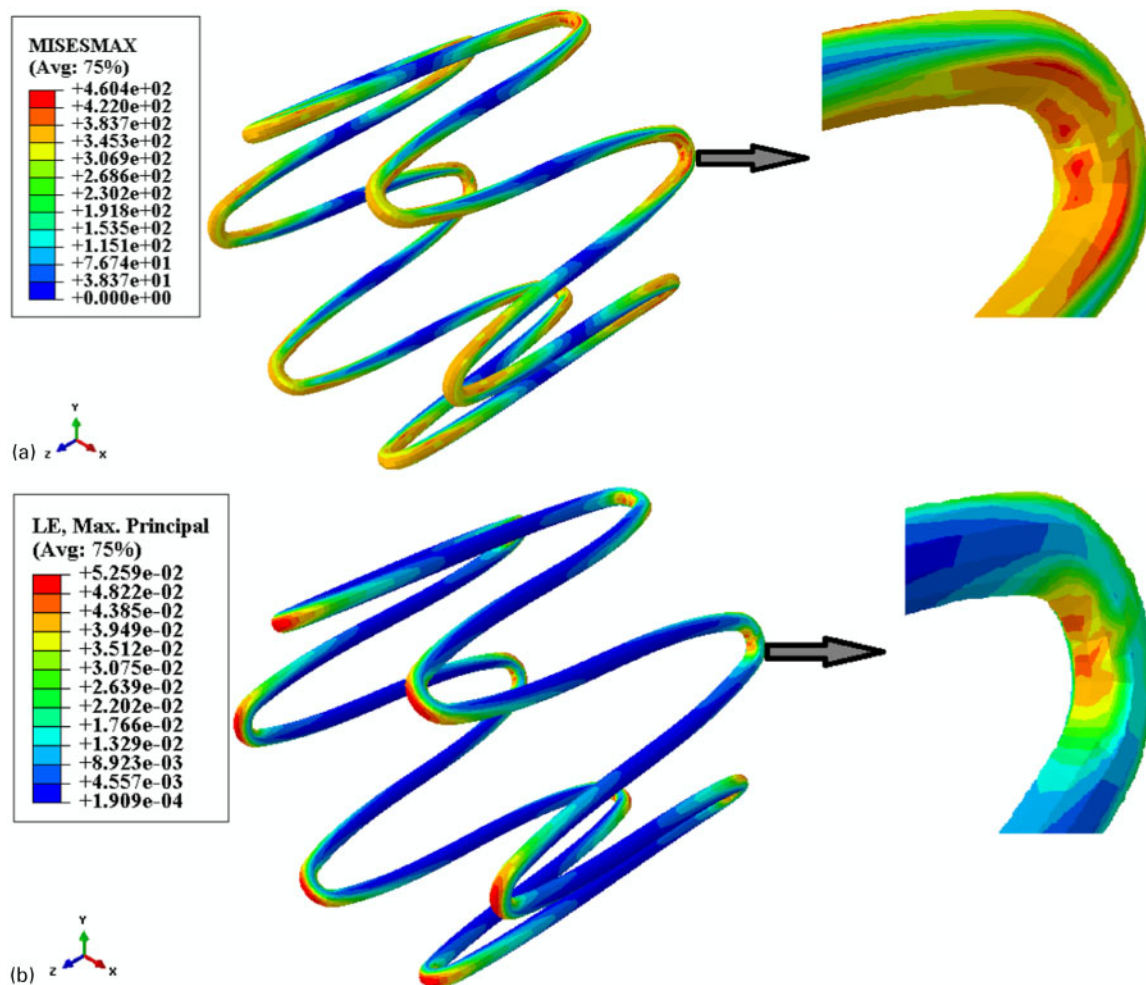
Equal 60% crimping of the stents illustrated in Figs. 11a and 13a indicates no noticeable difference in radial displacements of samples 1 and 2.

Comparison of Figs. 11b and 13b indicates a 5.14% decrease in fractional conversion of austenite to martensite from 1.264 to 1.199.

Fractional conversion of austenite to martensite phase under stress in the internal curvature of the stent of Fig. 11b is larger than that of Fig. 13b which indicates higher stress focused on internal curvature of the former stent. Considering the properties of the materials indicated in Table 2 at 24 and 22°C respectively, there should be a different range of loading and unloading plateau stress. Lower A_f temperature of Nitinol alloys and the extensive loading and unloading stress levels are related to the superelastic behaviour of the used alloys. For A_f temperature difference of 7°C, there should be $\sim 50\%$ variation in stress level.^{5,6} Moreover, reducing A_f temperature results in an increase in the upper plateau stress.⁵²

Figure 14 shows an increase in upper plateau stress due to the difference between A_f temperature of 22 and 24°C. For A_f temperature difference of 2°C, a variation limit of 15% is expected which is confirmed by experimental and numerical results.^{5,6,13,16} Angular difference between stent geometry illustrated in Figs. 2 and 3 is only 1°. The basis for the aforementioned geometric design is the result of aging treatment of Ti–50.7%Ni alloy at 500°C and between 30 and 60 min time intervals.¹⁸ The stent shown in Fig. 2 reveals, however, more acceptable mechanical and practical performance in comparison with the stent illustrated in Fig. 3. Nevertheless, according to Fig. 3 and considering short segments of the stent and wider angle between the stent segments, better geometric conditions for crimping test may be expectable.^{10,12,47–49} Acceptable clinical and mechanical performance of the stent of Fig. 2 is at the same time mainly rooted in material properties like aging treatment (for Ti–50.7%Ni alloy at 500°C for 60 min) and 65° optimum geometric angle.¹⁸ As far as fractional martensite formation is concerned, the stent of Fig. 13b is sufficient to generate superelastic behaviour in comparison with the stent of Fig. 11b.

Figure 15 shows an increase in martensite formation due to the difference between A_f temperatures of 22 and 24°C. According to this figure, the distribution of the martensitic phase in the 65° stent shown in Fig. 13b is more normalised than the 66° stent shown in Fig. 11b. With complete martensitic phase and hysteresis loop formation, appropriate superelastic behaviour of the 65°



a maximum von Mises yield stress; b maximum principal strain; c radial displacement; d fraction of martensite
 12 Result of 60% crimping induced on biliary stent made with sample No. 2 of Table 2 having 65° angle

stent is assessable. Because of less COF, greater RRF, higher transformation strain, full mechanical hysteresis loop, well acquired superelastic behaviour, smaller stress concentration and maximum strain on the internal curvatures of the stent, the stent displayed in Fig. 2 is better than that shown in Fig. 3.

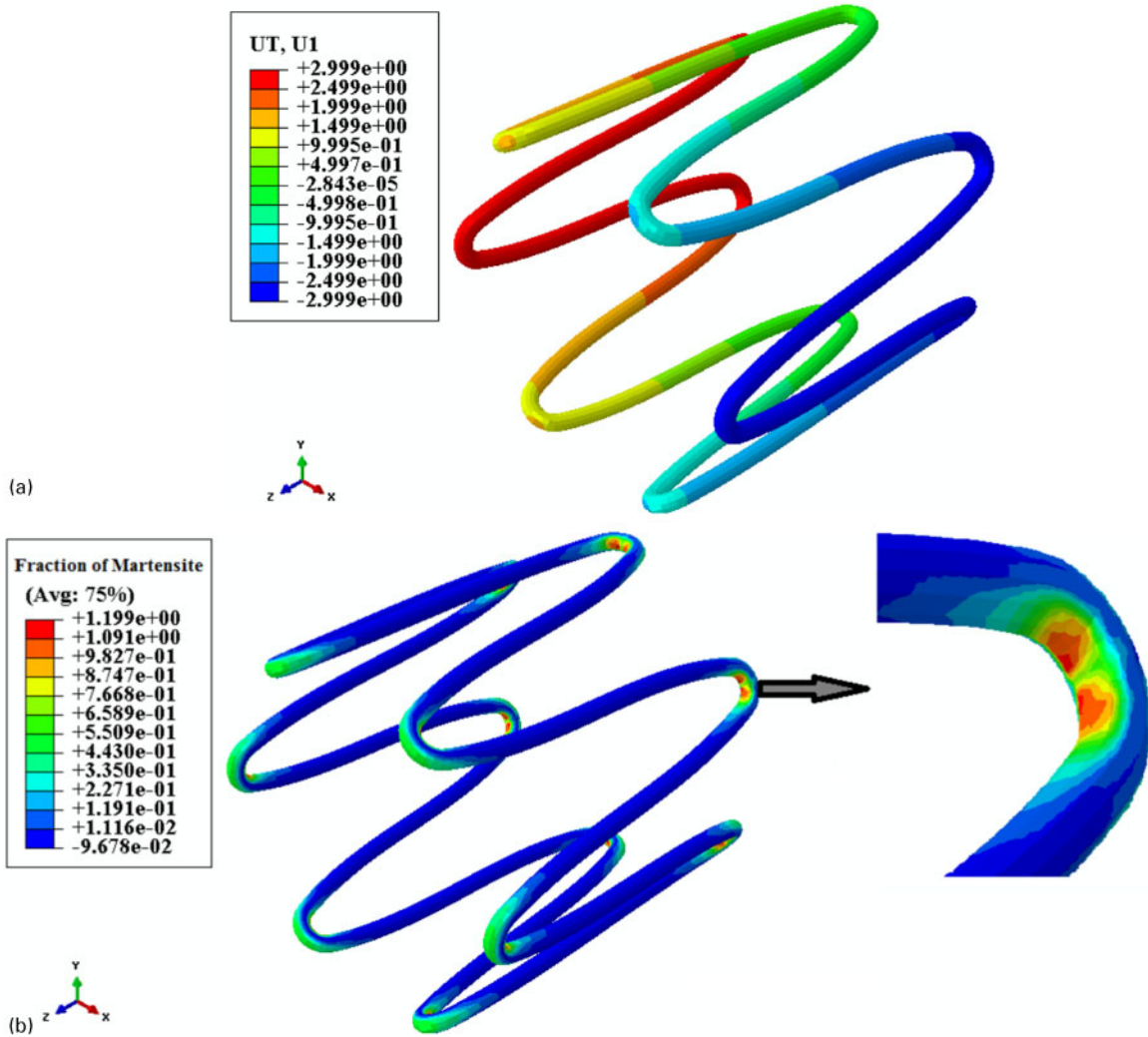
Limitations

This simulation is complex because of the existence of the contacts, non-linear geometry, material non-linearity, large deformation, additional buckling and bending of the stent. On the other hand, during crimping, self-contact phenomenon (contact between the edges of the stent) is anticipated which can impose additional stress on the contact points. However, according to Wu *et al.*,³⁹ owing to the superelasticity behaviour of the stent, these types of stresses can be neglected. Crimping tests have only been performed in radial orientations. It is obvious that more experiments and simulation results related to stenosis degree of ducts are needed to reach to a comprehensive conclusion.

Conclusions

Owing to good retrievability, flexibility and ease of manufacturing, the Z shape geometry is chosen for the

design of a new generation of biliary stents capable of exerting different amounts of radial displacements and stresses provided by Nitinol wires of appropriate superelastic behaviour. Finite element modelling employed to determine the effects of length and angle of the segments and the A_f temperature of the alloy indicates that the curved intersegments are the most critical regions bearing the highest levels of stress in the Nitinol biliary stents. The areas between two wire heads (parallel segments) bear the lowest level of stress. Maximum contraction forces are achieved at the highest critical stresses. The highest martensite fractional change occurs at the inside areas of the curved head segments as well as the areas with the highest stress concentrations; whereas the reduction in the length of the segments at wider angles is expected to yield better crimping results with more reasonable mechanical and clinical performance. Biliary Nitinol stents with optimal A_f temperature of 24°C and intersegment angle of 65° have the best mechanical performance for clinical applications under 60% crimp test. This is due to their lower COF, higher RRF and better superelastic behaviour than A_f temperature of 22°C and intersegment angle of 66°. Our model calculations showed that a 1° change in stent intersegment angle and 2°C change in A_f temperature could exert a substantial effect on the mechanical

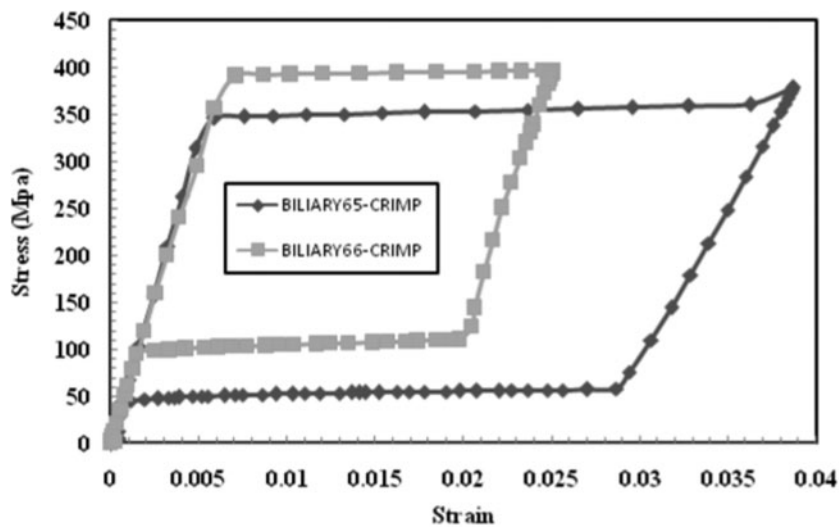


a radial displacement; b fraction of martensite

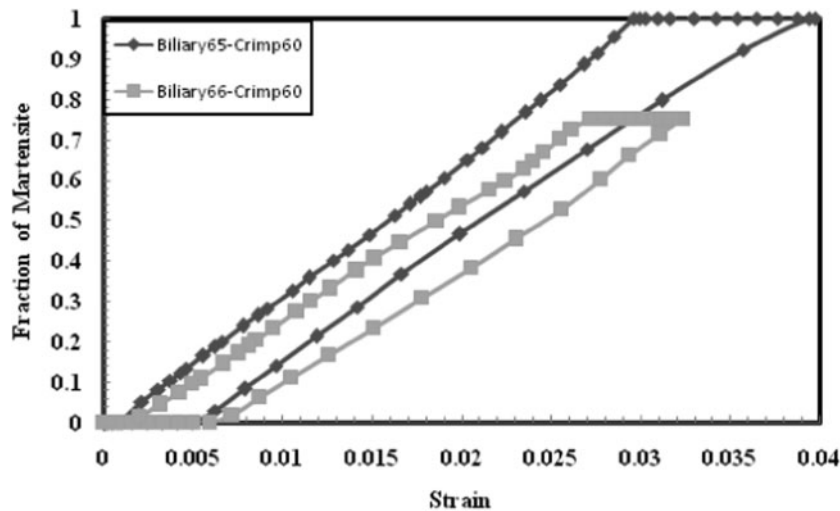
13 Result of 60% crimping induced on biliary stent made with sample No. 2 of Table 2 having 65° angle

performance of the Nitinol stent. This study showed that the optimisation of superelasticity and hysteresis behaviour of the Nitinol wires provides exceptional chance

for the exertion of appropriate force–displacement regimes required in stent placements prescribed for the treatment of gastrointestinal disorder.



14 Comparison of stress–strain curves for 60% crimped biliary stents having bending angles of 65 and 66°: material properties are listed in Table 2



15 Martensite formation due to 60% crimping of biliary stents having bending angles of 65 and 66°: material properties are listed in Table 2

Acknowledgements

The authors would like to thank Dr Amir R. Khoei, professor at the Civil Engineering Department, Sharif University of Technology and Mr Ehsan Haghghat, research assistant at McMaster University for assisting the implementation of the simulation programme to the modelled samples. They would also like to thank Mr S. M. Seyed Salehi and Mr H. G. Hosseinabadi, PhD Students at the Material Science and Engineering Department of Sharif University of Technology for his invaluable advises about the numerical analysis of the stents.

References

- A. Ganji, F. Malekzadeh, M. Safavi, S. Nasser Moghaddam, M. Nouraie, S. Merat, H. Vahedi, N. Zendehtel and R. Malekzadeh: *Middle East J. Digest. Dis.*, 2009, **1**, (2), 56–62.
- J. H. Ausubel, P. S. Meyer and I. K. Wernick: *Technol. Soc.*, 2001, **23**, (2), 131–146.
- H. Isayama, Y. Nakai, Y. Toyokawa, O. Togawa and C. Gon: *Gastrointest. Endosc.*, 2009, **70**, (1), 37–44.
- T. H. Baron: *Am. Soc. Gastrointest. Endosc.*, 2009, **17**, (2), 1–4.
- D. Stoeckel, A. R. Pelton and T. Duerig: *Eur. Radiol.*, 2004, **14**, 292–301.
- T. W. Duerig, D. E. Tolomeo and M. Wholey: *Min. Invas. Ther. Allied Technol.*, 2000, **9**, (3/4), 235–246.
- B. Patrick, B. S. Snowhill, L. N. John, L. S. Randall and H. S. Frederick: *Invest. Radiol.*, 2001, **36**, (9), 521–530.
- F. D. Whitcher: *Comput. Struct.*, 1997, **64**, (5–6), 1005–1011.
- L. Petrini, F. Migliavacca, P. Massarotti, S. Schievano, G. Dubini and F. Auricchio: *J. Biomech. Eng.*, 2005, **127**, 716–725.
- C. Kleinstreuer, Z. Li, C. A. Basciano, S. Seelecke and M. A. Farber: *J. Biomech.*, 2008, **41**, 2370–2378.
- H. V. D. Merwe, B. D. Reddy, P. Zilla, D. Bezuidenhout and T. Franz: *J. Biomech.*, 2008, **41**, 1302–1309.
- M. DeBeule, S. V. Cauter, P. Mortier, D. V. Loo, R. V. Impec, P. Verdonck and B. Verheghe: *Med. Eng. Phys.*, 2009, **31**, 448–453.
- G. Silber, M. Alizadeh and A. Aghajani: *Int. J. Energy Technol.*, 2010, **2**, (19), 1–7.
- Y. Liu and P. Galvin: *Acta Mater.*, 1997, **45**, (11), 4431–4439.
- A. R. Pelton, J. DiCello and S. Miyazaki: *Minim. Invas. Ther. Allied Technol.*, 2000, **9**, (1), 107–118.
- K. Koop, D. Lootz, C. Kranz, C. Momma, B. Becher and M. Kieckbusch: *Progr. Biomed. Res.*, 2001, **6**, (3), 237–245.
- A. R. Pelton, T. Duerig and D. Stockel: *Min. Invas. Ther. Allied Technol.*, 2004, **13**, (4), 218–221.
- X. Liu, Y. Wang, D. Yang and M. Qi: *Mater. Character.*, 2008, **59**, 402–406.
- E. Henderson, D. H. Nash and W. M. Dempster: *J. Mech. Behav. Biomed. Mater.*, 2011, **4**, (3), 261–268.
- F. Migliavacca, L. Petrini, P. Massarotti, S. Schievano, F. Auricchio and G. Dubini: *Biomech. Model. Mechanobiol.*, 2004, **2**, (4), 205–217.
- P. Terriault, V. Brailovski and R. Gallo: *J. Biomech.*, 2006, **39**, (15), 2837–2844.
- F. Auricchio, M. Conti, M. D. Beule, G. D. Santis and B. Verheghe: *Med. Eng. Phys.*, 2011, **33**, 281–289.
- F. Auricchio and R. L. Taylor: *Comput. Methods Appl. Mech. Eng.*, 1997, **143**, (1–2), 175–194.
- M. Conti, M. D. Beule, P. Mortier, D. V. Loo, P. Verdonck, F. Vermassen, P. Segers, F. Auricchio and B. Verheghe: *J. Mater. Eng. Perform.*, 2009, **18**, 787–792.
- N. Rebelo, N. Walker and H. Foadian: *Abaqus User's Conf.*, 2001, **143**, 421–434.
- F. Auricchio and R. Taylor: *Comput. Methods Appl. Mech. Eng.*, 1996, **143**, 175–194.
- J. Lubliner and F. Auricchio: *Int. J. Solids Struct.*, 1996, **33**, 991–1003.
- F. Auricchio, A. Coda, A. Reali and M. Urbano: *J. Mater. Eng. Perform.*, 2009, **18**, 649–654.
- J. Arghavani, F. Auricchio, R. Naghdabadi and S. Sohrabpour: *Int. J. Plast.*, 2010, **26**, 976–991.
- J. Khalil-Allafi, X. Ren and G. Eggeler: *Acta Mater.*, 2002, **50**, 793–803.
- A. G. Prince, G. L. Quarini, J. E. Morgan and J. Finlay: *Mater. Sci. Technol.*, 2003, **19**, 561–565.
- J. Eaton-Evans, J. M. Dulieu-Barton, E. G. Little and I. A. Brown: *Appl. Mech. Mater.*, 2005, **3–4**, 47–52.
- J. Eaton-Evans, J. M. Dulieu-Barton, E. G. Little and I. A. Brown: *J. Strain Anal.*, 2006, **41**, 481–495.
- J. Eaton-Evans, J. M. Dulieu-Barton, E. G. Little and I. A. Brown: *J. ASTM Int.*, 2006, **3**, 1–12.
- J. M. Dulieu-Barton, J. Eaton-Evans, E. G. Little and I. A. Brown: *Strain*, 2008, **44**, 102–118.
- T. Belytschko, W. K. Liu and B. Moran: 'Nonlinear finite elements for continua and structures'; 2000, New York, Wiley.
- F. Auricchio, M. Conti, S. Morganti and A. Reali: *CMES*, 2010, **57**, (3), 225–243.
- A. Farnoush, Q. Li: 'Three Dimensional Nonlinear Finite Element Analysis of the Newly Designed Cardiovascular Stent', 5th Australasian Congress on Applied Mechanics (ACAM), Brisbane, Australia, December 2007, 10–12.
- W. Wu, M. Qi, X. Liu, D. Yang and W. Wang: *J. Biomech.*, 2007, **40**, (13), 3034–3040.
- X. Gong, T. Duerig, A. R. Pelton, N. Rebelo, K. Perry: 'Finite element analysis and experimental evaluation of superelastic Nitinol stents', In Proceedings of the International Conference on Shape Memory and Superelastic Technology (SMST), Monterey, CA, USA, 2003, 1–11.
- L. Petrini, F. Migliavacca, P. Massarotti, S. Schievano, G. Dubini and F. Auricchio: *J. Biomech. Eng.*, 2005, **127**, 716–725.

42. M. Salaheldin, S. P. Zilla and T. Franz: *Cardiovasc. Eng. Technol.*, 2010, **1**, (4), 269–281.
43. V. Gideon, P. Kumar and L. Mathew: *Trends Biomater. Artif. Organs*, 2009, **23**, (1), 16–20.
44. N. B. Morgan: *Mater. Sci. Eng. A*, 2004, **A378**, 16–23.
45. A. R. Pelton, V. Schroeder, M. R. Mitchell, X. Y. Gong, M. Barneya and S. W. Robertson: *J. Mech. Behav. Biomed. Mater.*, 2008, **1**, 153–164.
46. M. Santillo: 'Master's dissertation, Fracture and crack propagation study of a Superficial Femoral Artery Nitinol stent', Pavia University, Lombardy, Italy, 2008.
47. R. Wang and K. Ravi-Chandar: *J. Appl. Mech.*, 2004, **71**, 697–705.
48. R. Wang and K. Ravi-Chandar: *J. Appl. Mech.*, 2004, **71**, 706–712.
49. S. Canic, K. Ravi-Chandar, Z. Krajcer, D. Mirkovic and S. Lapin: *Tex Heart Inst. J.*, 2005, **32**, (4), 502–506.
50. K. Otsuka and T. Kakeshita: *MRS Bull.*, 2002, **27**, (2), 91–98.
51. J. Khalil-Allafi, G. Eggeler, A. Dlouhy, W. Schmahl and C. Somsen: *Mater. Sci. Eng. A*, 2004, **A378**, 148–151.
52. M. Patel, D. Plumley and R. Bouthot: 'The Effects of Varying Active A_f Temperatures on the Fatigue Properties of Nitinol Wire', ASM Material and Process Conference and For Medical Devices Exposition (MPMD), Boston, MA, USA, November 2005, 1–8.